Properties of sintered glass-ceramics in the diopside–albite system

Alexander Karamanov [a,*], Lorenzo Arrizza [b], Ildiko Matekovits [c], Mario Pelino [a]

[a] *Department of Chemical Engineering and Materials, University of L'Aquila, Monteluco di Roio 67100, Italy*
[b] *Microscopy Centrum, University of L'Aquila, Monteluco di Roio 67100, Italy*
[c] *Department of Materials and Chemical Engineering, Politecnico di Torino, 10129 Turin, Italy*

Abstract

A series of sintered glass-ceramics belonging to the system diopside–albite, forming by surface crystallization 30, 50 and 65% diopside, was investigated. In order to study the effect of bulk crystallization on the sintering a 0.7% of Cr_2O_3 as nucleation agent was added in one of the compositions.

The crystallization was evaluated by DTA and density measurements and the degree of densification by the linear shrinkage and total porosity. These results were confirmed by SEM and XRD, respectively. The mechanical properties of the final glass-ceramics were measured and discussed as a function of the percentage of crystal phase formed and kind of crystallization (i.e., surface or bulk).
© 2004 Elsevier Ltd and Techna S.r.l. All rights reserved.

Keywords: A. Sintering; D. Glass-ceramics

1. Introduction

The first work on sintered glass-ceramics was published by Sack in 1957 [1]; only few years after Stookey's discovery of the controlled nucleation and crystallization of glass-ceramics [2–4]. However, as noted by McMillan [5], the sinter-crystallization was used even at the end of the XIX century. In 1896, Garchy produced artificial stone by heat-treatment of pressed soda-lime-silica scrap glass. The obtained blocks were used as pavement in some streets of Paris and lasted for many years.

During the sinter-crystallization process the nucleation is surface induced, so that no nucleating agents or thermal steps are required; the heat-treatment, producing sintered glass-ceramics, is usually shorter. By using ceramic forming techniques (powder pressing and slip castings) glass-ceramics with complicated shapes can be obtained [2–4], while the sintering of glass frit, placed loosely in refractory moulds, produces large tiles (up to $2\,m^2$) with a marble and granite-like appearance [2,3,6,7]. The glass-ceramics solders and coatings [2–4] may also be considered as sintered glass-ceramics.

In the present work sintered glass-ceramics, forming different percent of crystal phase and belonging to the diopside ($CaO \cdot MgO \cdot 2SiO_2$)–albite ($Na_2O \cdot Al_2O_3 \cdot 6SiO_2$) system are presented. The publication highlights the final structure of the materials as well the properties of the glass-ceramics obtained.

The phase diagram of diopside–albite pseudo binary system [8] shows a large and a narrow crystallization fields for diopside and albite, respectively, indicating big differences in the crystallization trends of the two phases. Practically, only diopside formation is expected while the residual glass retains a composition similar to albite. The different crystallization behavior may be explained in terms of crystal structures: the albite has a complicated framework structure, while diopside has the simple chain structure of the monoclinic pyroxene [9].

Due to the big density difference between the crystal and amorphous structure [10–12] without nucleation agents the diopside is formed only by surface crystallization. However, when appropriate nucleating agents are used, a consistent diposide bulk crystallization can be attained [2–4,13–15]. A typical nucleation agent is Cr_2O_3 which promotes fast spinel precipitation; the fine spinel crystals become nuclei for epitaxial pyroxene growth. Cr_2O_3 has low solubility in silicate melts [16] and its optimal concentration as nucleation agent

* Corresponding author. Tel.: +39-0862-434233;
fax: +39-0862-434233.
E-mail address: karama@ing.univaq.it (A. Karamanov).

is relatively low (about 0.7 wt.%) inducing insignificant variation in the glass composition [4,14,15].

2. Experimental

A series of glass batches were prepared by mixing quartz sand ($SiO_2 > 99.5\%$) and technically pure $Al(OH)_3$, $CaCO_3$, $MgCO_3$ and Na_2CO_3. The corresponding theoretical compositions (labeled G1, G2 and G3) are reported in Table 1, together with the values, obtained after melting, by XRF analysis (Spectro XEPOS); both results shown a good agreement. The diopside–albite phase diagram [8] and the theoretical compositions are shown in Fig. 1.

In order to study the effect of bulk nucleation on sinter-crystallization, a 0.7 wt.% Cr_2O_3 was added to G2 thus obtaining G2-Cr composition.

The melting of the glasses was carried out in 500 ml corundum crucibles at 1500 °C for 2 h. The melts were fritted and the obtained frit (about 200–220 g for each glass) was broken, milled and sieved. The milling was carried out in agate mill using portions of 50–60 g frit and 20 min milling at 300 turns per minute (t.p.m.). In the present study the fraction below 75 μm was used.

The crystallization was evaluated in the 20–1300 °C temperature interval by DTA at 10 °C/min using about 100 mg of powder samples.

The "green" samples with initial sizes 10/10/10 and 50/4/3 mm³ were prepared by mixing the glass powders with 7.5% PVA solution and by pressing at 150 MPa. After drying and a 30 min holding at 270 °C (to eliminate the PVA), the samples were heated to 800 °C at 20 °C/min (temperature below crystallization DTA onsets) and sintered for 2 h; the temperature was then increased at 5 °C/min to 900 °C and after the 1 h crystallization step the samples were cooled at 10 °C/min.

The degree of sintering was evaluated by the liner shrinkage and by the porosity of the final glass-ceramics. The linear shrinkage, related to the initial size of 50 mm, was

Table 1
Chemical compositions of the investigated glasses (mol%); t, theoretical, a, analyzed

	G1		G2		G2-Cr		G3	
	t	a	t	a	t	a	t	a
SiO_2	54	53.0	58	55.1	58	54.8	62	61.9
Al_2O_3	2	2.1	4	3.9	4	3.6	6	4.9
Cr_2O_3					0.3	0.3		
CaO	21	22.1	17	19.3	17	19.6	13	13.6
MgO	21	20.6	17	17.8	17	17.6	13	13.2
Na_2O	2	2.2	4	3.9	4	4.1	6	6.4

measured by micrometer (with uncertainly of ±0.025 mm) while the porosity, P, was evaluated by the difference between absolute density, ρ_{gc}, and apparent densities, ρ_a, of glass-ceramics:

$$P = 100 \times \frac{\rho_{gc} - \rho_a}{\rho_{gc}} \quad (1)$$

ρ_a were estimated by a dry flow Pycnometer (GeoPyc 1360) while ρ_{gc} by He displacement Pycnometer (AccyPyc 1330), after crashing and milling the samples below 45 mm. The experimental associated error in evaluation of P was estimated as ±0.3%.

The crystalline fraction, x (wt.%), was evaluated by density measurements through the following equation [12]:

$$x = 100 \times \frac{1/\rho_g - 1/\rho_{gc}}{1/\rho_{g(cr)} - 1/\rho_{cr}} \quad (2)$$

where ρ_g is the absolute density of parent glass, $\rho_{g(cr)}$ is the density of a hypothetical glass with the composition of the formed crystal phase and ρ_{cr} is the density of the crystal phase.

In the method, it is assumed that the volume of the parent glass, V_g, consists of two parts: $V_{g(cr)}$—with the composition of the crystal phase which is going to be formed and $V_{g(r)}$—with the composition of the residual glass. Then, during crystallization, only the $V_{g(cr)}$ part is transformed in the crystal phase with volume V_{cr}. A detailed description of the
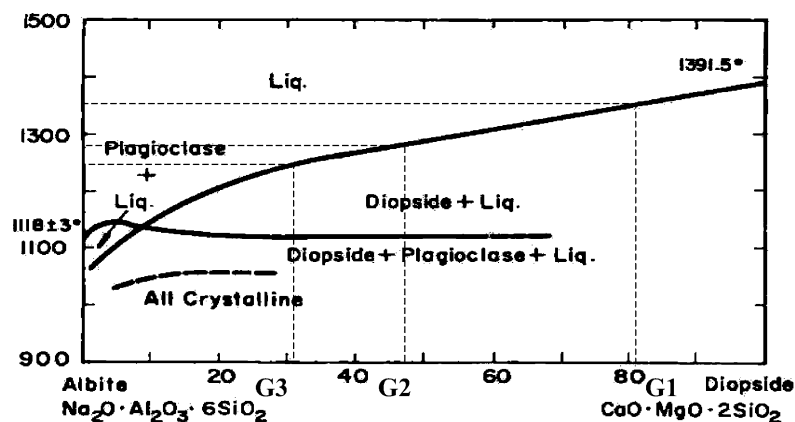

Fig. 1. Phase diagram of the system diopside–albite [8] with the theoretical G1, G2 and G3 compositions.

methodological approach and application to the crystallization of glasses is reported elsewhere [12].

In the case of diopside ρ_{cr} and $\rho_{g(cr)}$ have values of 3.27 and 2.75 g/cm³, respectively. The experimental associated error to the measurements of ρ_g and ρ_{gc} was evaluated as ± 0.003 g/cm³, which corresponds to an error of $\pm 1\%$ crystal phase.

A series of five samples of each glass-ceramic was used for the evaluation of the mechanical properties: the Young modulus was measured by means of the non-destructive resonance frequency technique (Grindosonic) while the bending strength was evaluated by a three point bending test with 40 mm outer span and a speed of 0.1 mm/min (SINTEC D/10). The Vickers hardness (at 50 N loading) was estimated after polishing by using a WOLPERT apparatus. The thermal expansion coefficient of glass-ceramics was evaluated in the 20–300 °C temperature interval by a Differential Dilatometer (Netzsch 402 ED) at 5 °C/min.

The morphology of the fractured final glass-ceramics was examined by Scanning Electron Microscopy (Philips XL30CP).

3. Results and discussion

Fig. 2 shows the viscosity–temperature curves of the investigated compositions, calculated by Lacatos method [17]. The viscosity curves of the investigated glasses are very similar in the sinter-crystallization range. This justifies the use of identical sintering heat-treatment and explains the crystallization trends only by the differences in the chemical compositions with respect to the phase diagram.
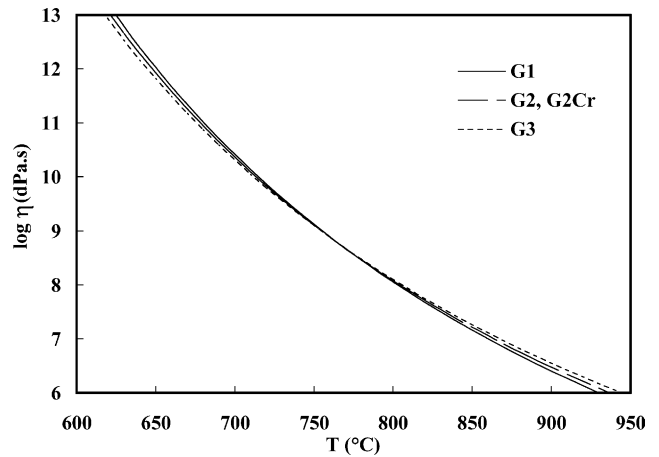

Fig. 2. The hypothetical viscous–temperature curves of G1, G2 and G3, calculated by Lacatos method.

The DTA curves of the investigated glasses are plotted in Fig. 3. The glass transition temperatures, T_g, are similar, which confirm that the viscosity is not significantly influenced by the variation of the composition. The liquidus temperatures, T_l, of G1, G2 and G3 are in good agreement with the phase diagram (see Fig. 1) while the addition of Cr_2O_3 in G2-Cr increases T_l. The crystallization peak temperatures, T_p, decrease and the intensity of crystallization peaks increase as a function of the amount of crystal phase formed. In the case of G2-Cr, T_p decreases by 20 °C compared to G2, which demonstrates the efficiency of Cr_2O_3 as nucleating agent.

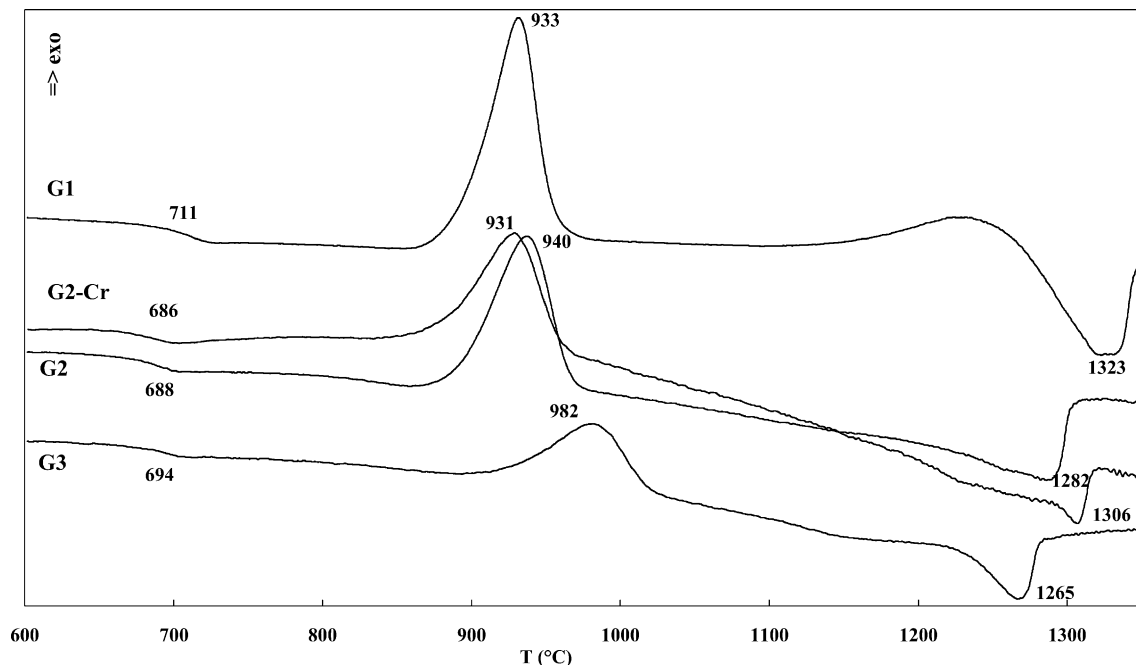The bulk nucleation in G2-Cr and the surface crystallization in G1, G2 and G3 were confirmed by additional

Fig. 3. DTA traces of the investigated compositions at 10 °C/min.

Table 2
Liner shrinkages, absolute, ρ_{gc}, and apparent, ρ_a, densities of glass-ceramics and absolute densities of parent glasses, ρ_g, together with the corresponding percentages of porosity and crystal phase formed

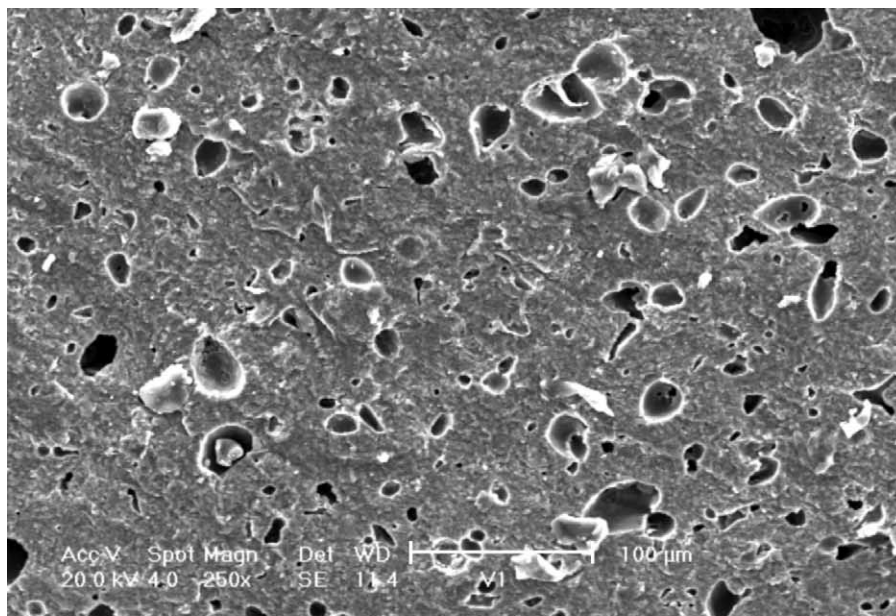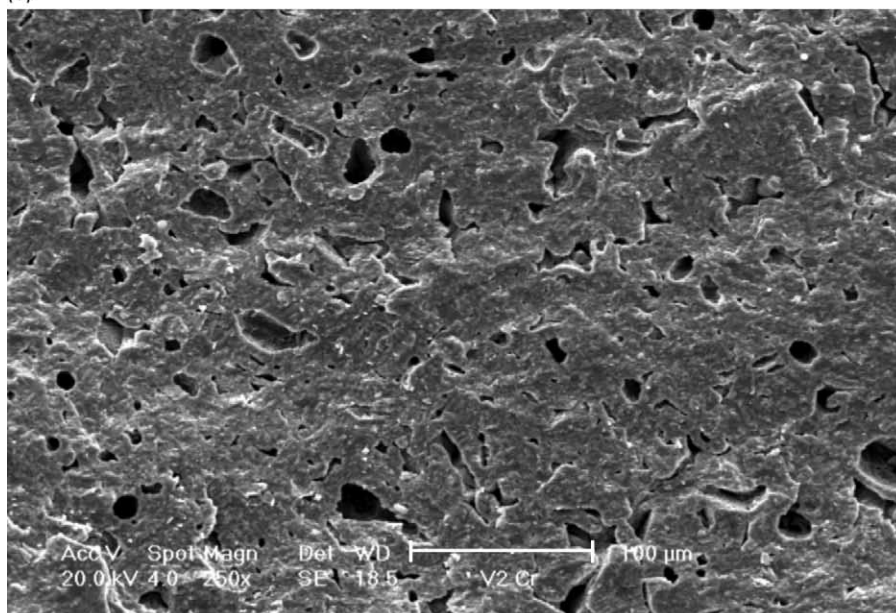|	Liner shrinkage (%)	ρ_a	ρ_g	ρ_{gc}	Porosity (%)	Crystal phase (wt.%)
G1	13.7	2.73	2.743	3.066	11	64
G2	13.8	2.66	2.687	2.924	8	50
G3	14.1	2.58	2.558	2.679	4	29
G2-Cr	12.6	2.57	2.694	2.972	14	58
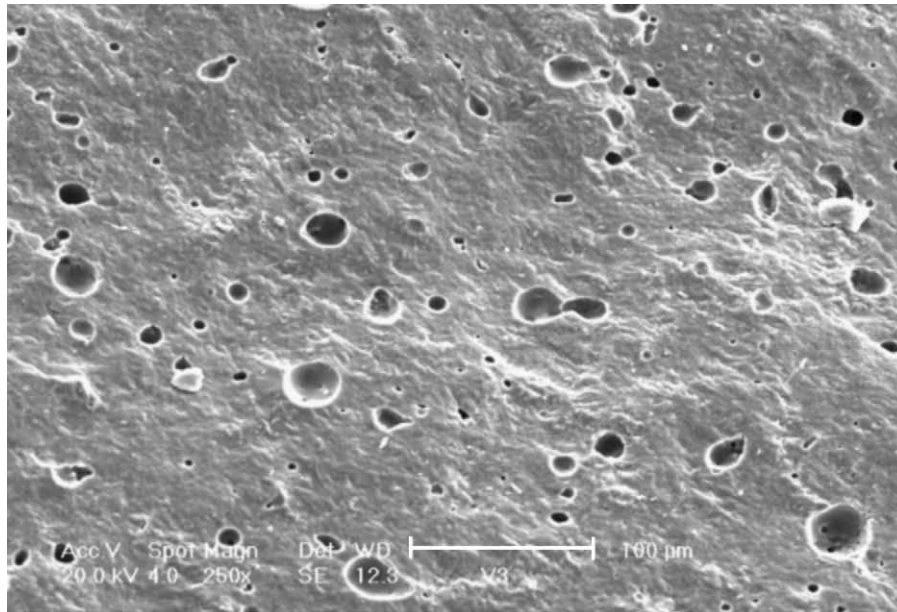
(a)
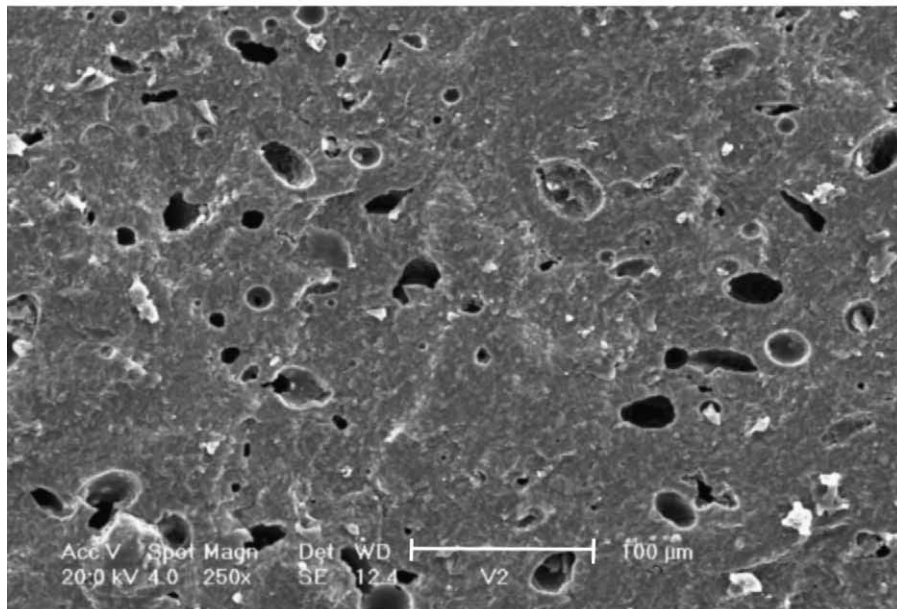
(b)

Fig. 4. SEM images of fractures of the glass-ceramics: (a) G3; (b) G2; (c) G3; and (d) G2-Cr.

(c)

(d)

Fig. 4. (*Continued*).

DTA experiments. The samples of each composition were heated at 10 °C/min to the nucleation temperature, 750 °C (i.e., 40–60 °C higher than T_g), hold for 1 h and then heated at the same heating rate to 1000 °C. In G2-Cr T_p decreases by 10 °C, while in the other glasses it remains without variations.

The DTA result highlighted that intensive crystallization process occurs in the 850–950 °C interval, so the

Table 3
Properties of obtained glass-ceramics

	Bending strength (MPa)	Modulus of elasticity (GPa)	Vickers hardness (HV)	Thermal expansion ($\times 10^{-7}$ deg^{-1})
G1	131 ± 11	112 ± 8	70	84.7
G2	120 ± 13	104 ± 7	69	86.7
G3	111 ± 12	91 ± 4	66	87.6
G2-Cr	96 ± 13	82 ± 8	41	78.3

sintering and crystallization temperatures were selected as 800 °C (2 h) and 900 °C (1 h), respectively.

The XRD spectra of the parent glasses were completely amorphous, while the analysis of final glass-ceramics highlighted only diopside formation.

The results of the linear shrinkage, absolute and apparent densities of glass-ceramics and absolute density of parent glasses are summarized in Table 2, together with the percentages of porosity and diopside formed, evaluated by Eqs. (1) and (2), respectively.
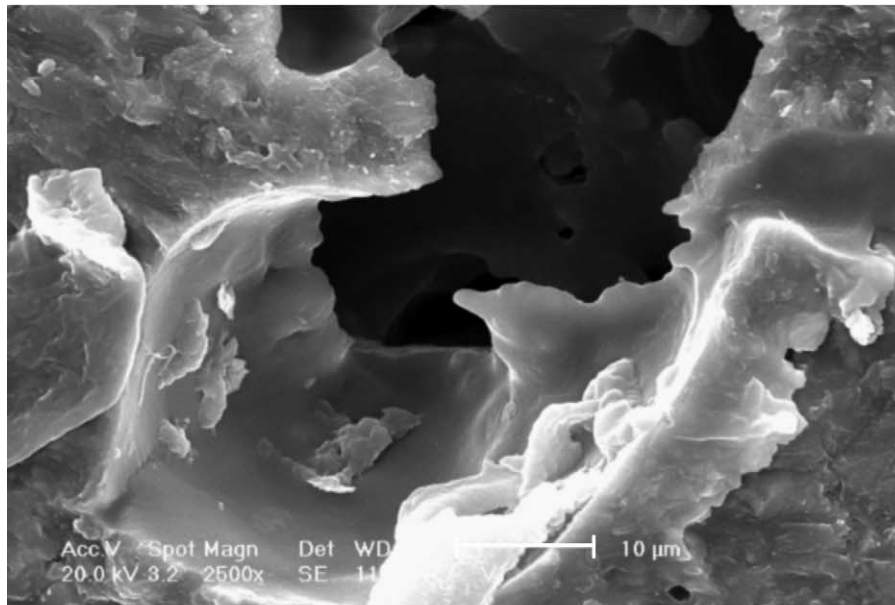
The amounts of crystal phase formed in G3 and G2-Cr are comparable to the values of the phase diagram, assuming that

that all CaO and MgO form diopside and that the residual glass has an albite composition. In G1 and G2 the amounts of crystal phase is lower than that expected by the phase diagram so that in these glass-ceramics part of CaO and MgO remains in the residual glassy phase.

The linear shrinkages of G1, G2 and G3 are comparable (between 13.7 and 14.1%) while G2-Cr shows a lower value (12.6%), indicating an inferior degree of densification. This conclusion is confirmed by the porosity evaluation, where the maximum porosity percentage of 14% is obtained for G2-Cr, compared to 8% for G2. The minor densification in G2-Cr may be attributed to the intensive phase
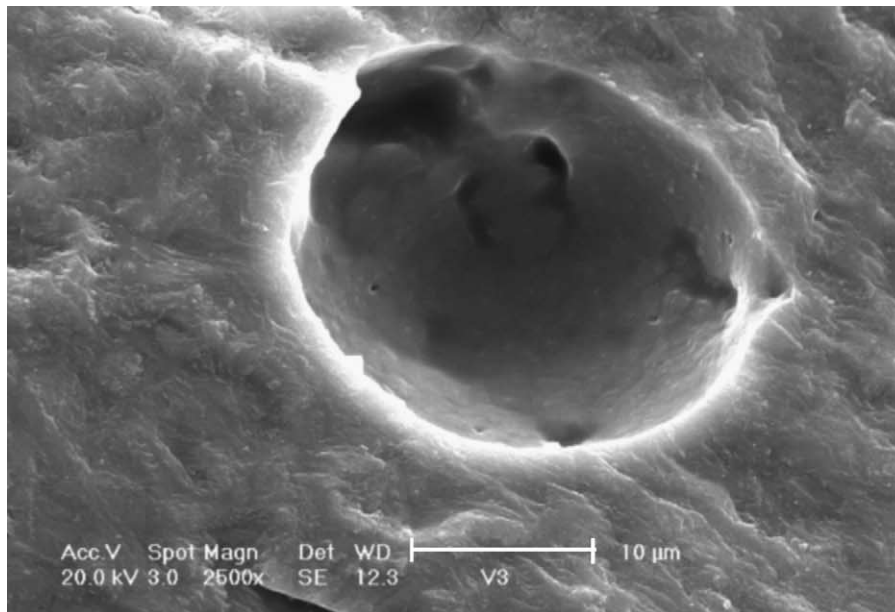
(a)

(b)

Fig. 5. Closed porosity in G3 (a) and open porosity in G1 (b).

formation due to the bulk crystallization, which inhibits the densification.

In G1, G2 and G3 the porosity increases as a function of the amount of crystal phase formed. This, however, cannot be explained only with the increasing of the crystallization rate because the final glass-ceramics have similar shrinkage values. Some additional porosity might be formed during phase formation due to the significant volume variation, related to diopside crystallization.

Fig. 4 shows SEM images of fractures of the glass-ceramics. SEM observations confirm the results of porosity evaluation and highlight that the porosity varies with the increasing of the crystallization trend. The structure of G3 (Fig. 4a) is based only on closed porosity with clear spherical form, in G2 (Fig. 4b) and G1 (Fig. 4c) open porosity is also evident, while in G2-Cr (Fig. 4d) the porosity is predominantly open. Fig. 5a demonstrated a typical closed porous in G3, while Fig. 5b highlighted open porosity in G1.

In Table 3 the properties of the obtained glass-ceramics are summarized. In G1, G2 and G3 the properties improve as function of the amount of diopside formed, while in G2-Cr the higher residual porosity due to intensive bulk crystallization leads to a decrease in the characteristics.

Notwithstanding the low temperature heat-treatment (2 h at $800\,^\circ$C and 1 h at $900\,^\circ$C) the overall properties may be considered as very high. Similar, even lower characteristics are reported for many non-porous glass-ceramics, produced by bulk nucleation and crystallization, as well as for sintered glass-ceramics obtained at higher temperatures [2–5].

This is the result of relatively low porosity, of resistant diopside crystal and albite amorphous phases in the final materials, as well as of the similar thermal expansion coefficients of the crystal and glassy phases, as is indicated by the similar thermal expansion coefficients of the glass-ceramics.

4. Conclusions

The results highlighted that sintered glass-ceramics with high mechanical properties may be synthesized in the diopside–albite system.

The properties improve with the increasing of the percentage of diopside formed, even if the increasing of the crystalline phase leads to higher porosity in the final glass-ceramics. With percentages of crystal phase up to 30% the porosity is closed while at higher percentages of 50–65% formation of open porosity takes place.

The additions of Cr_2O_3 induces bulk nucleation, and thus increases the phase formation rate and inhibits the densifica-

tions. As a result the porosity increases and the mechanical properties decrease.

References

[1] I. Gutzow, J. Shmelzer, The Vitreous State—Structure, Thermodynamics, Rheology and Crystallisation, Springer-Verlag, Berlin, New York, 1995.

[2] Z. Strnad, Glass-Ceramic Materials, Elsevier, Amsterdam, 1986.

[3] W. Höland, G. Beall, Glass-Ceramics Technology, The American Ceramics Society, Westerville, 2002.

[4] N. M. Pavlushin, Chemical Technology of Glass and Glass-Ceramics, Strojizdat, Moskow, 1983 (in Russian).

[5] P.W. McMillan, Glass-Ceramics, Academic Press Inc., London, 1979.

[6] S. Nakamura, Crystallized glass article having a surface pattern, US Patent 3,955,989 (11 May 1976).

[7] A. Karamanov, I. Gutzow, I. Penkov, Diopside marble-like glass-ceramics, Glastech. Ber., Glass Sci. Tech. 67 (7) (1994) 202–209.

[8] J.F. Schairer, H.S. Yoder Jr., Nature of residual liquids from crystallization, with data on the system nepheline-diopside silica, Am. J. Sci. 258A (Bradley Vol.) (1960) 273–283.

[9] W. Deer, R. Howie, J. Zussman, An Introduction to the Rock-Forming Minerals, Longman Scientific & Technical, 1992.

[10] E.D. Zanotto, E.A. Muler, A simple method to predict the nucleation mechanism in glass (Letter to the Editor), J. Non-Cryst. Solids 130 (1991) 220–221.

[11] J. Schmelzer, J. Moller, I. Gutzow, R. Pascova, R. Muller, W. Pannhorst, Surface energy and structure effects on surface crystallization, J. Non-Cryst. Solids 183 (1995) 215–223.

[12] A. Karamanov, M. Pelino, Evaluation of the degree of crystallisation in glass-ceramics by density measurements, J. Eur. Ceram. Soc. 19 (5) (1999) 649–654.

[13] R.D. Rawlings, Production and properties of silceram glass-ceramic, in: Glass-Ceramic Materials—Fundamentals and Applications, Series of Monographs on Material Science, Engineering and Technology, Mucchi Editore, 1997, pp. 115–133.

[14] A. Karamanov, P. Pisciella, M. Pelino, The effect of Cr_2O_3 as nucleating agent in iron rich glass-ceramics, J. Eur. Ceram. Soc. 19 (15) (1999) 2641–2645.

[15] L.A. Zhunina, M.I. Kuzmenkov, L.W. Yaglov, Pyroxene Glass-Ceramics, Belorrussia Government University, Minsk, 1974 (in Russian).

[16] M.L. Keith, Phase equilibria in the system $MgO–Cr_2O_3–SiO_2$, J. Am. Ceram. Soc. 37 (10) (1954) 490–496.

[17] H. Scholze, Glass Nature, Structure and Properties, Springer-Verlag, Berlin, 1990.